Combined PCMRI and CFD hemodynamics in a flow-model and in the thoracic aorta

A. F. Stalder[1,2], Z. Liu[3], R. Lorenz[2], J. Hennig[2,4], J. G. Korvink[4,5], and M. Markl[2]

[1]Dept. of Radiology, Xuanwu Hospital, Capital Medical University, Beijing, China, People's Republic of, [2]Dept. of Diagnostic Radiology - Medical Physics, University Hospital, Freiburg, Germany, [3]Changchun Institute of Optics, Fine Mechanics and Physics (CIOMP), Chinese Academy of Science, Changchun, China, People's Republic of, [4]Freiburg Institute for Advanced Studies (FRIAS), Freiburg, Germany, [5]Dept. of Microsystems Engineering, University of Freiburg, Germany

Introduction: Both flow-sensitive 4D MRI and computational fluid dynamics (CFD) have successfully been applied to analyze complex 3D flow patterns in the cardiovascular system. However, both modalities suffer from limitations related to spatio-temporal resolution, measurement errors, and noise (MRI) or incomplete model assumptions and boundary conditions (CFD) (1,2). The aim of this study was to directly compare the results of flow-sensitive 4D MRI and CFD in a simple model system *in vitro* and more complex blood 3D flow in the thoracic aorta *in vivo*. Finally, the potential of the method is illustrated using a very fine boundary layer mesh to derive detailed maps of vessel wall parameters.

Methods: Data was acquired using a 3T MR system (Magnetom TRIO, Siemens, Germany 8-channel receive coil) with a 4D flow-sensitive MRI sequence in a flow model *in vitro* and an healthy volunteer *in vivo*. The flow model consisted in a rigid PVC tube with 3.4 cm inner-diameter connected to a clinical bloodpump-system (Deltastream DP2, Medos, Stolberg, Germany) that produced a constant (nonpulsatile) flow of contrast agent (Gd-BOPTA, Multihance, Bracco) doped distilled water at 37°C. The 3D flow-sensitive MRI acquisition parameters were: Voxel size 0.4×0.4×0.6 mm^3, venc 0.5 m/s, TE / TR 4.62 / 8 ms, Bandwidth 440 Hz/pixel, α 13°.The thoracic aorta of a young healthy volunteer (age: 26, male) was imaged after injection of a blood pool contrast agent (MS325, Vasovist; Schering AG) using a respiration controlled and ECG gated 4D flow-sensitive MRI sequence (3) (spatial resolution: 2.82x1.67x3.5 mm^3, temporal resolution: 48.8 ms, venc: 1.5 m/s, TE / TR 3.67 / 6.1 ms, Bandwidth 480 Hz/pixel, α 13°). Phase contrast angiography (4)(*in vitro* model) and contrast-enhanced MRA (*in vivo* model) were calculated and used for subvoxel resolution segmentation using level-set active contours (5). The resulting smooth geometries were used to create meshes. The tube model mesh consisted in 163'000 subdomain elements. In order to asses wall parameters reliably (6,7), a very fine boundary layer mesh was used for the thoracic aorta model (242'000 elements: subdomain elements and 6 boundary layers with an initial layer thickness of 10 μm and a stretching factor of 1.2). The flow-sensitive 4D MRI data was used to define inflow boundary conditions which matched the *in vivo* situation (plane1, Fig.3). In addition, null-pressure at the outlet plane and no-slip on the vessel wall were used as boundary conditions. CFD was performed using a commercial finite element solver (Comsol Multiphysics v3.4, Comsol Inc., Burlington, MA, USA, www.comsol.com) based on a direct linear solver (PARDISO). Blood was assumed to be incompressible with a density of 1050 kg/m^3 and a dynamic viscosity of 0.0045 Pa·s (8). The model was solved over 5 cardiac cycles.

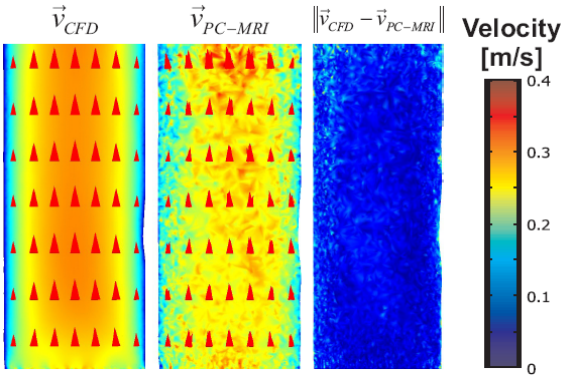

Fig.1: Flow velocities in the tube model calculated using CFD and measured using PC-MRI.

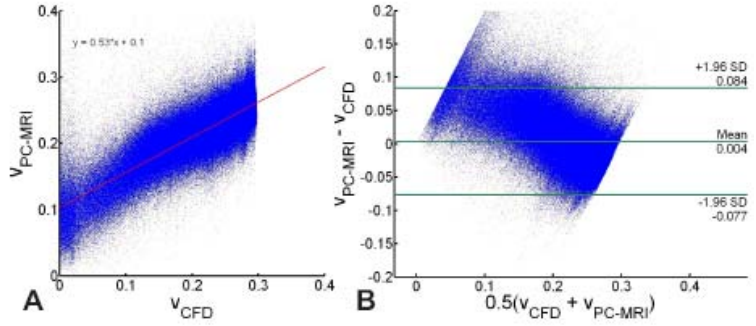

Fig.2: CFD vs. PC-MRI velocities in the tube model: Scatter plot (A) and Bland-Altman plot (B).

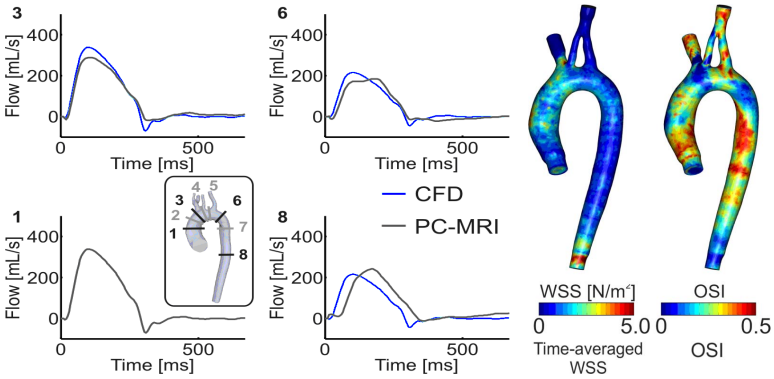

Fig.3: Blood flow in the thoracic aorta model derived from PCMRI and CFD.

Fig.4: CFD-based time-averaged WSS and OSI

Results: While the velocities measured in the tube model *in vitro* using flow-sensitive MRI presented visible noise and near-parabolic distributions (Fig.1), the velocities based on CFD were parabolic without apparent noise. The overall absolute error between both modalities in the model *in vitro* was limited but PC-MRI tended to underestimate and overestimate peak velocities and low-velocities, respectively (Fig.2). A direct comparison of flow-time curves between CFD and PC-MRI at four planes along the thoracic aorta model is shown in Fig.3. As CFD assumed rigid walls and incompressible fluids, all CFD flow-time curves had the same shape (but different amplitudes). The flow-curves for PC-MRI at planes 3, 6 and particularly 8, appeared delayed compared to the flow dynamics simulated by CFD. Indeed, the aortic compliance *in vivo* is expected to delay flow wave propagation compared to stiff walls as used for the CFD calculations. Detailed CFD based calculation of Wall Shear Stress (WSS) and Oscillatory Shear Index (OSI) maps on the thoracic aorta model (Fig.4) reveal the presence of proatherosclerotic low WSS and high OSI zones (proximal descending aorta, branches).

Discussion & Outlook: To date, there is no gold standard for the assessment of 4D blood flow hemodynamics *in vivo*. On one hand, PC-MRI can directly measure hemodynamics *in vivo* but suffers from measurement errors and limited resolution (Fig.1-2). On the other hand, CFD depends on the validity of the hemodynamic models (e.g. compliance, Fig.3). By comparing both modalities within a single framework, discrepancies were observed but the overall patterns were coherent. If adequate methods are used (e.g. patient-specific boundary conditions, fine boundary layer mesh (7)) CFD can compute very accurate flow and vessel wall parameters such as WSS and OSI (Fig.4). The combination of 4D flow-sensitive MRI and CFD may be used to refine both methodologies (noise for MRI, model accuracy for CFD) which may help to enhance the assessment and understanding of blood flow *in vivo*.

References: 1.Stalder AF. PhD Thesis, University Freiburg 2009 2.Stalder AF, et al. Proc. 16th ISMRM, Toronto, Canada: 2008 3.Markl M, et al. J Magn Reson Imaging 2007;25 4.Bock J, et al. Proc. 20th Conf MRA, Graz, Austria: 2008 5.Yushkevich PA, et al. Neuroimage 2006;31 6.Prakash S, et al. J Biomech Eng 2001;123 7.Hazer D, et al. Proc. Curac, Karlsruhe, Germany: 2007 8.Gnasso A, et al. Circulation 1996;94

Acknowledgements: Deutsche Forschungsgemeinschaft (DFG), Grant # MA 2383/4-1; Bundesministerium für Bildung und Forschung (BMBF), Grant # 01EV0706. EU Science & Technology Fellowship Program, Ref# EuropeAid/127024/L/ACT/CN_STF/33